NASA TECHNICAL NOTE

NASA TN D-3163

DRAG CHARACTERISTICS OF A SERIES OF LOW-DRAG BODIES OF REVOLUTION AT MACH NUMBERS FROM 0.6 TO 4.0

by Roy V. Harris, Jr., and Emma Jean Landrum

Langley Research Center
Langley Station, Hampton, Va.

NATIONAL AERONAUTICS AND SPACE ADMINISTRATION • WASHINGTON, D. C. • DECEMBER 1965

DRAG CHARACTERISTICS OF A SERIES OF LOW-DRAG BODIES OF REVOLUTION AT MACH NUMBERS FROM 0.6 TO 4.0

By Roy V. Harris, Jr., and Emma Jean Landrum

Langley Research Center
Langley Station, Hampton, Va.

NATIONAL AERONAUTICS AND SPACE ADMINISTRATION

For sale by the Clearinghouse for Federal Scientific and Technical Information
Springfield, Virginia 22151 – Price $2.00

DRAG CHARACTERISTICS OF A SERIES OF LOW-DRAG BODIES OF REVOLUTION AT MACH NUMBERS FROM 0.6 TO 4.0

By Roy V. Harris, Jr., and Emma Jean Landrum
Langley Research Center

SUMMARY

An analytical and experimental study has been made of the drag characteristics of a series of low-drag bodies of revolution at Mach numbers from 0.6 to 4.0. The bodies considered in this study are length-volume Haack-Adams bodies and were derived, with the use of slender-body theory, to have a minimum wave drag for a given length, volume, and base area. Although the wave drag of these bodies can be considered as minimum only for that particular class of bodies which are either closed (zero base radius) or have zero surface slope at the base, it has been shown that the wave drag of these bodies is only slightly greater than that for the minimum-wave-drag body. When the body base area is zero, the Haack-Adams bodies are identical with the Sears-Haack bodies.

Wave-drag coefficients determined with the use of slender-body theory are in good agreement with the experimentally determined wave-drag coefficients near a Mach number of 1.0. However, as Mach number (M) is increased, the slender-body theory overestimates the body wave drag. These Mach number effects are greater at the lower fineness ratios. The slender-body theory gives good agreement near a Mach number of 1.0 because as the Mach number approaches 1.0 the fineness ratio becomes large with respect to $\sqrt{M^2 - 1}$ and the slender-body requirement is more nearly satisfied. At the higher Mach numbers, the body fineness ratio must be very large in order to satisfy the slender-body requirement. Computations in which the method of characteristics is used show good agreement with the experimental results.

In order that the turbulent skin-friction drag data could be compared on a convenient basis, the average skin-friction coefficients and corresponding Reynolds numbers were transformed to the incompressible case by the Sommer and Short T' method (NACA TN 3391). Most of these data, particularly at the lower transformed Reynolds numbers, fall above the Kármán-Schoenherr incompressible curve. At the higher transformed Reynolds numbers, the average skin-friction coefficients more nearly approach the Kármán-Schoenherr curve. This trend would be expected since at the higher transformed Reynolds numbers, the boundary-layer thickness is smaller with respect to the body radius and, hence, more nearly approaches the two-dimensional case.

INTRODUCTION

The ability to predict the drag of bodies of revolution has become increasingly important as a result of the emphasis being placed on high-speed missiles and aircraft in recent years. Of particular importance are the so-called Haack-Adams bodies of revolution (ref. 1) because they often are used as a basis for obtaining rapid estimates of body wave drag. When the body base area is zero, the Haack-Adams bodies are identical with the Sears-Haack bodies of revolution (refs. 2 and 3). The Haack-Adams bodies were derived by using slender-body theory in an attempt to define the body shapes for minimum wave drag. Although the wave drag of these bodies can be considered as minimum only for that particular class of bodies which are either closed (zero base radius) or have zero surface slope at the base, it has been shown that the wave drag of these bodies is only slightly greater than that for the minimum-wave-drag body (ref. 4).

Slender-body theory indicates that the wave drag of Haack-Adams bodies is invariant with Mach number. However, if the supersonic area rule is used in combination with slender-body theory in an attempt to account for the Mach number effects, it can be seen that there should be some wave-drag variation with Mach number for these bodies (ref. 5). In addition, it has been shown experimentally that the wave-drag coefficients for a series of Haack-Adams bodies with a fineness ratio of 8 do vary in the Mach number range from 1.6 to 2.4 and are less than that predicted by slender-body theory (ref. 6). Also, the results of skin-friction calculations for cones (ref. 7) indicate that the skin-friction drag of bodies of revolution will be slightly greater than that for the equivalent flat plate which is most often used as a basis for skin-friction drag predictions.

As a result of these considerations, a study has been made by analytical and experimental means to determine the drag characteristics over a wide range of Mach numbers and Reynolds numbers for a series of Haack-Adams bodies of revolution designed to have minimum wave drag for a given length, volume, and base area.

SYMBOLS

Measurements for this investigation were taken in the U.S. Customary System of Units. Equivalent values are indicated herein in the International System (SI) in the interest of promoting use of this system in future NASA reports. Details concerning the use of SI, together with physical constants and conversion factors, are given in reference 8.

A cross-sectional area, sq in. (meters^2)

$C_{D,w}$ wave-drag coefficient, $\frac{\text{Wave drag}}{qA_{max}}$

C_F^* transformed average skin-friction coefficient

C_p pressure coefficient, $\frac{p - p_\infty}{q}$

d diameter, in. (meters)

l length, in. (meters)

M free-stream Mach number

p local static pressure, lb/sq in. (newtons/meter^2)

p_∞ free-stream static pressure, lb/sq in. (newtons/meter^2)

q free-stream dynamic pressure, lb/sq in. (newtons/meter^2)

r radius, in. (meters)

R^* transformed Reynolds number based on body length

x distance along longitudinal axis of body, in. (meters)

Subscripts:

base base

max maximum

THEORETICAL CONSIDERATIONS

Slender-body theory, which was used in deriving the Haack-Adams body shapes of this investigation, is a special case of small-perturbation potential-flow theory with the additional restriction that the product $r\sqrt{M^2 - 1}$ is very much less than x (ref. 9). This theoretical approach indicates that for this class of bodies (i.e., bodies which have either zero base radius or zero surface slope at the base), the body wave drag is invariant with Mach number and depends only on the fineness ratio and degree of afterbody closure. The effects that are predicted by slender-body theory of fineness ratio and afterbody closure on the wave drag of length-volume Haack-Adams bodies (ref. 1) are shown in figure 1.

In order to examine the effects of Mach number on body wave drag for a wide range of body fineness ratios, pressure distributions were computed by the method of characteristics (ref. 10) for afterbody closure ratios of 0 and 0.532 and for body fineness ratios from 5 to 15. The calculations were made for Mach numbers of 1.5, 2.0, 2.5, 3.0, 3.5, and 4.0. The wave drag was obtained by integrating the computed pressure distribution over the body according to the following relation:

$$C_{D,w} = \int_0^l \frac{2C_p r}{r_{max}^2}\left(\frac{dr}{dx}\right)dx$$

The equations for body radius (derived from ref. 1) and wave-drag coefficient for the bodies with $A_{base}/A_{max} = 0$ are

$$\frac{r}{r_{max}} = \left[1 - \left(\frac{2x}{l} - 1\right)^2\right]^{3/4}$$

$$C_{D,w} = \int_0^l \frac{-6C_p}{l}\left(\frac{2x}{l} - 1\right)\left[1 - \left(\frac{2x}{l} - 1\right)^2\right]^{1/2} dx$$

The corresponding equations for the bodies with $A_{base}/A_{max} = 0.532$ are

$$\frac{r}{r_{max}} = \left\{0.70700\left[1 - \left(\frac{2x}{l} - 1\right)^2\right]^{3/2} + 0.16934\left(\frac{2x}{l} - 1\right)\left[1 - \left(\frac{2x}{l} - 1\right)^2\right]^{1/2} + 0.16934 \cos^{-1}\left(1 - \frac{2x}{l}\right)\right\}^{1/2}$$

$$C_{D,w} = \int_0^l -\frac{C_p}{l}\left[4.24200\left(\frac{2x}{l} - 1\right) - 0.67736\right]\left[1 - \left(\frac{2x}{l} - 1\right)^2\right]^{1/2} dx$$

The results of this analytical study, along with the corresponding results obtained with the use of slender-body theory, are shown in figures 2 and 3 for the afterbody closure ratios of 0 and 0.532, respectively. The characteristics theory indicates that body wave drag is not invariant with Mach number and approaches the slender-body theory with decreasing Mach number. Also, the Mach number effects are greater at the lower fineness ratios. Thus, it can be seen that slender-body theory overestimates the body wave drag, particularly at the low fineness ratios and high Mach numbers where the fineness ratio l/d_{max} is not very large with respect to $\sqrt{M^2 - 1}$ (i.e., where the slender-body restriction $r\sqrt{M^2 - 1} \ll x$ is not met).

EXPERIMENTS

Models

Haack-Adams bodies of revolution with fineness ratios of 7, 10, and 13 were constructed of aluminum for the afterbody closure ratios of 0 and 0.532. The longitudinal distributions of body radii are shown in figure 4 for each

series. Photographs of the models are presented in figure 5, and the ordinates are given in table I.

The theoretical length of each of the bodies with $A_{base}/A_{max} = 0$ was 38.240, 39.670, and 41.400 inches (97.130, 100.762, and 105.156 cm) for the fineness ratios of 7, 10, and 13, respectively. In order to accommodate a sting-support system, these bodies were terminated at the longitudinal station which produced a base radius of 0.880 inch (2.235 cm) at an actual length of 36 inches (91.44 cm). Thus, the test models consisted of the forward 36 inches (91.44 cm) of the theoretical bodies. Since the requirement of a sting-support system for the test models eliminated the possibility of measuring the total drag of the theoretical bodies, only pressure models were constructed for the series with $A_{base}/A_{max} = 0$. Both force and pressure models were constructed for the bodies with $A_{base}/A_{max} = 0.532$.

Each of the pressure models had a single row of orifices along the length of the body. At the 7- and 26-inch (17.78- and 66.04-cm) stations, orifices were also located 90° apart around the bodies. The orifice locations are given in table II. The force models were constructed so that the bodies could be attached to the sting-support system by means of an internally mounted strain-gage balance.

Tests and Corrections

The tests were conducted in the Langley 8-foot transonic pressure tunnel, in the Langley 4- by 4-foot supersonic pressure tunnel, and in the high Mach number test section of the Langley Unitary Plan wind tunnel. The Mach number ranges for the tests in each of the wind tunnels were 0.60 to 1.20, 1.41 to 2.01, and 2.50 to 3.95, respectively. For all tests, the dewpoint in the test sections was maintained sufficiently low to insure negligible condensation effects.

Pressure tests.- The Reynolds number based on the body length of 36 inches (91.44 cm) at each test Mach number was as shown in the following table:

Mach number	Reynolds number
0.60	9.5×10^6
.80	11.4
.90	11.9
.95	12.2
1.00	12.4
1.03	12.4
1.20	12.7
1.61	12.8
2.01	11.1
2.50	9.0
2.96	9.0
3.95	9.0

All pressure data were obtained with the angles of attack and sideslip of the model adjusted to produce axially symmetric pressure distributions at the 7- and 26-inch (17.78- and 66.04-cm) stations. The pressure data obtained in the Langley 8-foot transonic pressure tunnel and the Langley 4- by 4-foot supersonic pressure tunnel were determined from photographs of the multiple-tube manometer boards to which the pressure leads from the model orifices were connected. In the Langley Unitary Plan wind tunnel, the pressure measurements were made by connecting the orifices to valves which sample 48 pressures in sequence on a single transducer. The transducer output was digitized and recorded on punch cards to expedite data reduction.

Force tests.- The force-test portion of the investigation was performed for the bodies with $A_{base}/A_{max} = 0.532$ only. The tunnel stagnation pressure was varied at each Mach number in order to obtain data for a wide range of Reynolds numbers. All the force data were obtained with angles of attack and sideslip of the model adjusted to produce zero normal force and zero side force. The forces acting on the bodies of revolution were measured by means of a sting-supported six-component strain-gage balance mounted within the models. The base pressures were measured by means of a static-pressure orifice located within the model base cavity, and the measured drag forces were adjusted to correspond to a base pressure equal to free-stream static pressure.

Boundary-layer transition was fixed on the force models by placing 1/8-inch-wide (0.318-cm) roughness strips around the bodies at the 1/2-inch (1.27-cm) station. For the tests in the Langley 8-foot transonic pressure tunnel and in the Langley 4- by 4-foot supersonic pressure tunnel, the roughness particles consisted of No. 80 carborundum grit. For the tests in the Langley Unitary Plan wind tunnel, the roughness particles were No. 60 carborundum grit.

RESULTS AND DISCUSSION

Pressure Distributions

The measured surface pressure coefficients for the bodies of revolution with $A_{base}/A_{max} = 0$ are presented in table III. The experimental surface pressure coefficients are compared with those from characteristics theory at a Mach number of 2.01 in figure 6. Table IV presents the measured surface pressure coefficients for the bodies with $A_{base}/A_{max} = 0.532$. The surface pressure coefficients for those Mach numbers at which comparisons could be made with the characteristics theory are shown with the theory in figure 7. As might be expected, the limited comparisons shown in figures 6 and 7 indicate good agreement between the experimental pressure distributions and those determined by the method of characteristics.

Wave Drag

Experimental wave-drag coefficients have been determined for the bodies with $A_{base}/A_{max} = 0.532$ by integrating the measured surface pressure

coefficients. Figure 8 presents a comparison between the experimental wave-drag variation with Mach number and that indicated by the method of characteristics for the fineness ratios of 7, 10, and 13. Also shown are the drag levels indicated by slender-body theory. The results obtained with the use of the characteristics theory show excellent agreement with the experimental results, and the slender body theory gives good agreement near a Mach number of 1.0. However, as Mach number is increased, the slender-body theory overestimates the body wave drag. It should also be noted that the effects of Mach number are greater at the lower fineness ratios. The slender-body theory gives good agreement near a Mach number of 1.0 because as the Mach number approaches 1.0 the fineness ratio becomes large with respect to $\sqrt{M^2 - 1}$ and the slender-body requirement is more nearly satisfied. At the higher Mach numbers, the body fineness ratio must be very large in order to satisfy the slender-body requirement.

Skin-Friction Drag

The turbulent skin-friction drag coefficients have been determined for the bodies with $A_{base}/A_{max} = 0.532$ by subtracting the experimental pressure drag from the measured drag. In order that these data could be compared on a convenient basis, the resulting turbulent average skin-friction coefficients and the corresponding values of Reynolds number based on body length have been transformed to the incompressible case by the Sommer and Short T' method (refs. 11 and 12). The transformed skin-friction coefficients C_F^* and Reynolds numbers R^* for the various Mach numbers and fineness ratios are compared with the Kármán-Schoenherr incompressible curve in figure 9.

Most of the data, particularly at the lower transformed Reynolds numbers, fall above the Kármán-Schoenherr curve. This trend would be expected since the Kármán-Schoenherr formula was derived by using two-dimensional (flat-plate) relations. At the higher values of the transformed Reynolds number, the average skin-friction coefficients more nearly approach the Kármán-Schoenherr curve. This trend would also be expected since at the higher transformed Reynolds numbers, the boundary-layer thickness is smaller with respect to the body radius and, hence, more nearly approaches the two-dimensional case.

CONCLUDING REMARKS

The results of an analytical and experimental study of the drag characteristics of a series of low-drag bodies of revolution at Mach numbers from 0.6 to 4.0 warrant the following concluding remarks.

Wave-drag coefficients determined with the use of slender-body theory (i.e., small-perturbation potential-flow theory with the additional restriction that the product of the body radius r and the Prandtl-Glauert factor $\sqrt{M^2 - 1}$ is very much less than the distance along the longitudinal axis of the body) are

in good agreement with the experimentally determined wave-drag coefficients near a Mach number of 1.0. However, as Mach number M is increased, the slender-body theory overestimates the body wave drag. These Mach number effects are greater at the lower fineness ratios. The slender-body theory gives good agreement near a Mach number of 1.0 because as the Mach number approaches 1.0 the fineness ratio becomes large with respect to $\sqrt{M^2 - 1}$ and the slender-body requirement is more nearly satisfied. At the higher Mach numbers, the body fineness ratio must be very large in order to satisfy the slender-body requirement. Computations in which the method of characteristics is used show good agreement with the experimental results.

Most of the experimental transformed turbulent average skin-friction coefficients fall above the Kármán-Schoenherr incompressible curve at the lower transformed Reynolds numbers. At the higher transformed Reynolds numbers, the average skin-friction coefficients more nearly approach the Kármán-Schoenherr curve. This trend would be expected since at the higher transformed Reynolds numbers, the boundary-layer thickness is smaller with respect to the body radius and, hence, more nearly approaches the two-dimensional case.

Langley Research Center,
National Aeronautics and Space Administration,
Langley Station, Hampton, Va., August 17, 1965.

REFERENCES

1. Adams, Mac C.: Determination of Shapes of Boattail Bodies of Revolution for Minimum Wave Drag. NACA TN 2550, 1951.

2. Haack, W.: Projectile Shapes for Smallest Wave Drag. Translation No. A9-T-3, Contract W33-038-ac-15004(16351), ATI No. 27736, Air Materiel Command, U.S. Air Force, Brown Univ., 1948.

3. Sears, William R.: On Projectiles of Minimum Wave Drag. Quart. Appl. Math., vol. IV, no. 4, Jan. 1947, pp. 361-366.

4. Harder, Keith C.; and Rennemann, Conrad, Jr.: On Boattail Bodies of Revolution Having Minimum Wave Drag. NACA Rept. 1271, 1956. (Supersedes NACA TN 3478.)

5. Harris, Roy V., Jr.: An Analysis and Correlation of Aircraft Wave Drag. NASA TM X-947, 1964.

6. Bromm, August F., Jr.; and Goodwin, Julia M.: Investigation at Supersonic Speeds of the Wave Drag of Seven Boattail Bodies of Revolution Designed for Minimum Wave Drag. NACA TN 3054, 1953.

7. Bertram, Mitchel H.: Calculations of Compressible Average Turbulent Skin Friction. NASA TR R-123, 1962.

8. Mechtly, E. A.: The International System of Units – Physical Constants and Conversion Factors. NASA SP-7012, 1964.

9. Liepmann, H. W.; and Roshko, A.: Elements of Gasdynamics. John Wiley & Sons, Inc., c.1957, pp. 218-251.

10. Ferri, Antonio: Application of the Method of Characteristics to Supersonic Rotational Flow. NACA Rept. 841, 1946. (Supersedes NACA TN 1135.)

11. Sommer, Simon C.; and Short, Barbara J.: Free-Flight Measurements of Turbulent-Boundary-Layer Skin Friction in the Presence of Severe Aerodynamic Heating at Mach Numbers From 2.8 to 7.0. NACA TN 3391, 1955.

12. Peterson, John B., Jr.: A Comparison of Experimental and Theoretical Results for the Compressible Turbulent-Boundary-Layer Skin Friction With Zero Pressure Gradient. NASA TN D-1795, 1963.

TABLE I.- MODEL ORDINATES

(a) U.S. Customary Units

x, in.	r in inches for l/d_{max} =					
	7	10	13	7	10	13
	A_{base}/A_{max} = 0			A_{base}/A_{max} = 0.532		
0	0	0	0	0	0	0
.100	.089	.063	.049	.077	.054	.042
.200	.149	.106	.082	.131	.092	.071
.300	.202	.143	.111	.180	.126	.097
.400	.252	.177	.138	.223	.156	.120
.500	.296	.209	.163	.264	.185	.142
.600	.339	.239	.186	.302	.212	.163
.700	.379	.268	.208	.338	.237	.182
.800	.418	.296	.230	.373	.261	.201
.900	.456	.322	.251	.407	.285	.219
1.000	.492	.348	.271	.440	.308	.237
1.500	.661	.467	.364	.590	.413	.318
2.000	.811	.574	.447	.725	.508	.391
3.000	1.077	.763	.595	.964	.675	.519
4.000	1.308	.927	.723	1.172	.821	.631
5.000	1.512	1.073	.838	1.357	.950	.731
6.000	1.695	1.204	.941	1.524	1.067	.820
7.000	1.858	1.321	1.034	1.674	1.171	.901
8.000	2.004	1.426	1.117	1.808	1.266	.974
9.000	2.135	1.521	1.190	1.930	1.351	1.039
10.000	2.251	1.606	1.261	2.041	1.429	1.099
11.000	2.353	1.681	1.322	2.137	1.496	1.151
12.000	2.442	1.747	1.376	2.227	1.557	1.197
13.000	2.519	1.805	1.424	2.300	1.610	1.238
14.000	2.584	1.854	1.465	2.366	1.656	1.274
15.000	2.636	1.895	1.501	2.423	1.696	1.305
16.000	2.677	1.929	1.530	2.470	1.729	1.330
17.000	2.706	1.954	1.554	2.507	1.755	1.350
18.000	2.725	1.972	1.572	2.537	1.776	1.366
19.000	2.732	1.982	1.584	2.557	1.790	1.377
20.000	2.727	1.985	1.591	2.568	1.798	1.383
21.000	2.712	1.980	1.592	2.571	1.800	1.385
22.000	2.685	1.968	1.588	2.566	1.796	1.382
23.000	2.647	1.947	1.578	2.555	1.787	1.375
24.000	2.597	1.920	1.562	2.532	1.772	1.363
25.000	2.536	1.884	1.540	2.503	1.752	1.348
26.000	2.462	1.840	1.513	2.466	1.726	1.328
27.000	2.376	1.789	1.480	2.422	1.695	1.304
28.000	2.277	1.728	1.441	2.371	1.660	1.277
29.000	2.164	1.659	1.396	2.314	1.620	1.246
30.000	2.037	1.581	1.345	2.251	1.576	1.212
31.000	1.895	1.494	1.286	2.184	1.529	1.176
32.000	1.736	1.396	1.221	2.113	1.479	1.138
33.000	1.558	1.287	1.149	2.042	1.429	1.099
33.500				2.006	1.404	1.080
34.000	1.360	1.166	1.068	1.973	1.381	1.062
34.500				1.941	1.359	1.045
35.000	1.136	1.031	.979	1.912	1.339	1.030
35.500				1.889	1.322	1.017
36.000	.880	.880	.880	1.876	1.313	1.010
37.000	.577	.709	.770			
38.000	.173	.512	.648			
38.240	0					
39.000		.268	.509			
39.670		0				
41.400			0			

TABLE I.- MODEL ORDINATES - Concluded

(b) SI Units

x, cm	r in centimeters for l/d_{max} =					
	7	10	13	7	10	13
	A_{base}/A_{max} = 0			A_{base}/A_{max} = 0.532		
0	0	0	0	0	0	0
.254	.226	.160	.124	.196	.137	.107
.508	.378	.269	.208	.333	.234	.180
.762	.513	.363	.282	.457	.320	.246
1.016	.640	.450	.351	.566	.396	.305
1.270	.752	.531	.414	.671	.470	.361
1.524	.861	.607	.472	.767	.538	.414
1.778	.963	.681	.528	.859	.602	.462
2.032	1.062	.752	.584	.947	.663	.511
2.286	1.158	.818	.638	1.034	.724	.556
2.540	1.250	.884	.688	1.118	.782	.602
3.810	1.679	1.186	.925	1.499	1.049	.808
5.080	2.060	1.458	1.135	1.842	1.290	.993
7.620	2.736	1.938	1.511	2.449	1.715	1.318
10.160	3.322	2.355	1.836	2.977	2.085	1.603
12.700	3.840	2.725	2.129	3.447	2.413	1.857
15.240	4.305	3.058	2.390	3.871	2.710	2.083
17.780	4.719	3.355	2.626	4.252	2.974	2.289
20.320	5.090	3.622	2.837	4.592	3.216	2.474
22.860	5.423	3.863	3.023	4.902	3.432	2.639
25.400	5.718	4.079	3.203	5.184	3.630	2.791
27.940	5.977	4.270	3.358	5.428	3.800	2.924
30.480	6.203	4.437	3.495	5.657	3.955	3.040
33.020	6.398	4.585	3.617	5.842	4.089	3.145
35.560	6.563	4.709	3.721	6.010	4.206	3.236
38.100	6.695	4.813	3.813	6.154	4.308	3.315
40.640	6.800	4.900	3.886	6.274	4.392	3.378
43.180	6.873	4.963	3.947	6.368	4.458	3.429
45.720	6.922	5.009	3.993	6.444	4.511	3.470
48.260	6.939	5.034	4.023	6.495	4.547	3.498
50.800	6.927	5.042	4.041	6.523	4.567	3.513
53.340	6.888	5.029	4.044	6.530	4.572	3.518
55.880	6.820	4.999	4.034	6.518	4.562	3.510
58.420	6.723	4.945	4.008	6.490	4.539	3.493
60.960	6.596	4.877	3.967	6.431	4.501	3.462
63.500	6.441	4.785	3.912	6.358	4.450	3.424
66.040	6.253	4.674	3.843	6.264	4.384	3.373
68.580	6.035	4.544	3.759	6.152	4.305	3.312
71.120	5.784	4.389	3.660	6.022	4.216	3.244
73.660	5.497	4.214	3.546	5.878	4.115	3.165
76.200	5.174	4.016	3.416	5.718	4.003	3.078
78.740	4.813	3.795	3.266	5.547	3.884	2.987
81.280	4.409	3.546	3.101	5.367	3.757	2.891
83.820	3.957	3.269	2.918	5.187	3.630	2.791
85.090				5.095	3.566	2.743
86.360	3.454	2.962	2.713	5.011	3.508	2.697
87.630				4.930	3.452	2.654
88.900	2.885	2.619	2.487	4.856	3.401	2.616
90.170				4.798	3.358	2.583
91.440	2.235	2.235	2.235	4.765	3.335	2.565
93.980	1.466	1.801	1.956			
96.520	.439	1.300	1.646			
97.130	0					
99.060		.681	1.293			
100.762		0				
105.156			0			

TABLE II.- ORIFICE LOCATIONS

Orifice	x/l for l/d_{max} =					
	7	10	13	7	10	13
	A_{base}/A_{max} = 0			A_{base}/A_{max} = 0.532		
1	0.010	0.010	0.009	0.011	0.009	0.010
2	.016	.016	.015	.017	.017	.016
3	.023	.022	.021	.024	.023	.023
4	.035	.034	.032	.038	.038	.038
5	.052	.050	.048	.056	.055	.055
6	.078	.075	.072	.084	.083	.083
7	.105	.100	.096	.111	.111	.111
8	.131	.126	.121	.139	.138	.139
9	.157	.151	.144	.167	.166	.166
10	.183	.176	.168	.194	.194	.194
11	.183	.176	.169	.195	.194	.194
12	.183	.176	.168	.195	.193	.194
13	.183	.176	.169	.194	.194	.194
14	.235	.226	.217	.250	.222	.221
15	.288	.277	.265	.306	.249	.250
16	.340	.378	.361	.361	.277	.278
17	.392	.428	.409	.417	.305	.305
18	.444	.479	.457	.472	.416	.417
19	.497	.529	.502	.528	.472	.473
20	.549	.604	.578	.584	.528	.528
21	.628	.655	.626	.667	.583	.584
22	.681	.655	.626	.722	.666	.667
23	.681	.655	.626	.722	.722	.723
24	.680	.655	.626	.722	.723	.723
25	.680	.705	.674	.722	.722	.723
26	.733	.755	.723	.778	.723	.723
27	.785	.806	.771	.833	.778	.778
28	.838	.831	.795	.889	.834	.833
29	.864	.856	.819	.917	.889	.889
30	.890	.881	.843	.944	.917	.917
31	.917	.892	.853	.972	.945	.945
32	.927	.902	.863	.983	.972	.972
33	.937			.994	.984	.983
34					.995	.994
l, in.	38.240	39.670	41.400	36.000	36.000	36.000
l, cm	97.130	100.762	105.156	91.440	91.440	91.440

TABLE III.- PRESSURE COEFFICIENTS FOR THE BODY WITH $A_{base}/A_{max} = 0$

(a) $l/d_{max} = 7$

x/l	C_p for M =									x/l
	0.60	0.80	0.90	0.95	1.00	1.03	1.20	1.61	2.01	
0.010	0.375	0.417	0.453	0.482	0.523	0.561	0.551	0.444	0.415	0.010
.016	.325	.363	.398	.424	.464	.503	.501	.405	.354	.016
.023	.267	.300	.328	.355	.394	.436	.435	.368	.330	.023
.035	.191	.213	.235	.260	.299	.343	.329	.267	.249	.035
.052	.152	.171	.191	.213	.256	.298	.301	.229	.211	.052
.078	.098	.107	.119	.140	.179	.224	.217	.175	.161	.078
.105	.054	.054	.064	.079	.119	.163	.173	.145	.131	.105
.131	.026	.027	.030	.043	.082	.125	.136	.115	.103	.131
.157	.003	.002	.001	.011	.049	.092	.103	.093	.083	.157
.183	-.017	-.025	-.033	-.028	.005	.047	.077	.071	.065	.183
.235	-.037	-.048	-.061	-.059	-.021	.015	.044	.041	.037	.235
.288	-.061	-.076	-.095	-.106	-.071	-.031	.000	.013	.012	.288
.340	-.072	-.089	-.111	-.124	-.102	-.067	-.029	-.010	-.005	.340
.392	-.086	-.107	-.133	-.158	-.139	-.114	-.066	-.047	-.019	.392
.444	-.084	-.105	-.134	-.162	-.151	-.118	-.072	-.042	-.031	.444
.497	-.085	-.106	-.135	-.182	-.176	-.146	-.091	-.058	-.045	.497
.549	-.082	-.102	-.129	-.174	-.185	-.157	-.099	-.072	-.055	.549
.628	-.074	-.094	-.115	-.144	-.213	-.187	-.124	-.091	-.073	.628
.681	-.059	-.076	-.094	-.107	-.217	-.193	-.140	-.099	-.080	.681
.733	-.037	-.051	-.062	-.066	-.211	-.189	-.134	-.106	-.089	.733
.785	-.012	-.021	-.025	-.023	-.189	-.193	-.147	-.114	-.096	.785
.838	.013	.012	.017	.030	.078	-.182	-.150	-.120	-.101	.838
.864	.047	.050	.060	.075	.144	-.081	-.144	-.117	-.099	.864
.890	.086	.096	.112	.129	.193	.071	-.095	-.110	-.094	.890
.917	.140	.156	.175	.193	.237	.157	.064	-.067	-.086	.917
.927	.165	.186	.202	.221	.251	.173	.110	.015	-.074	.927
.937	.194	.215	.229	.246	.264	.185	.138	.071	-.005	.937

TABLE III.- PRESSURE COEFFICIENTS FOR THE BODY

WITH $A_{base}/A_{max} = 0$ - Continued

(b) $l/d_{max} = 10$

x/l	C_p for M =									x/l
	0.60	0.80	0.90	0.95	1.00	1.03	1.20	1.61	2.01	
0.010	0.214	0.230	0.255	0.276	0.313	0.347	0.289	0.252	0.226	0.010
.016	.199	.212	.232	.250	.285	.321	.288	.236	.194	.016
.022	.156	.163	.179	.196	.229	.267	.244	.208	.179	.022
.034	.113	.118	.126	.141	.172	.213	.166	.149	.130	.034
.050	.090	.090	.098	.109	.142	.184	.159	.140	.120	.050
.075	.062	.059	.063	.074	.103	.147	.121	.108	.092	.075
.100	.039	.031	.031	.038	.067	.110	.095	.083	.069	.100
.126	.019	.010	.006	.009	.034	.079	.071	.066	.053	.126
.151	.006	-.004	-.011	-.011	.005	.049	.052	.053	.043	.151
.176	.001	-.012	-.016	-.016	.005	.046	.040	.042	.032	.176
.226	-.014	-.031	-.039	-.043	-.033	.005	.016	.017	.011	.226
.277	-.022	-.039	-.049	-.058	-.040	-.009	.005	.013	.007	.277
.378	-.031	-.051	-.063	-.072	-.085	-.067	-.032	-.020	-.018	.378
.428	-.039	-.060	-.076	-.091	-.095	-.082	-.045	-.026	-.023	.428
.479	-.043	-.063	-.078	-.094	-.115	-.097	-.060	-.041	-.034	.479
.529	-.048	-.069	-.085	-.099	-.127	-.115	-.077	-.057		.529
.604	-.032	-.049	-.062	-.069	-.125	-.119	-.078	-.065	-.043	.604
.655	-.028	-.045	-.060	-.070	-.124	-.121	-.081	-.061	-.052	.655
.705	-.009	-.022	-.033	-.036	-.106	-.114	-.069	-.063	-.050	.705
.755	.003	-.009	-.015	-.016	.018	-.112	-.079	-.063	-.053	.755
.806	.024	.013	.011	.015	.062	-.107	-.080	-.066	-.052	.806
.831	.040	.031	.031	.040	.085	-.085	-.079	-.065	-.057	.831
.856	.061	.056	.059	.072	.113	-.007	-.067	-.057	-.056	.856
.881	.088	.087	.094	.108	.150	.114	-.031	-.051	-.052	.881
.892	.098	.102	.111	.125	.167	.152	-.008	-.046	-.047	.892
.902	.114	.117	.130	.145	.186	.182	.028		-.044	.902

TABLE III.- PRESSURE COEFFICIENTS FOR THE BODY

WITH $A_{base}/A_{max} = 0$ - Concluded

(c) $l/d_{max} = 13$

x/l	C_p for M =									x/l
	0.60	0.80	0.90	0.95	1.00	1.03	1.20	1.61	2.01	
0.009	0.170	0.185	0.196	0.228	0.260	0.282	0.262	0.212	0.182	0.009
.015	.148	.153	.154	.180	.207	.231	.209	.173	.156	.015
.021	.118	.119	.118	.144	.168	.192	.171	.131	.119	.021
.032	.079	.074	.076	.086	.107	.133	.096	.079	.079	.032
.048	.071	.066	.071	.079	.093	.125	.116	.083	.078	.048
.072	.062	.057	.056	.065	.083	.114	.089	.065	.060	.072
.096	.035	.029	.024	.030	.042	.073	.078	.057	.052	.096
.121	.023	.016	.010	.013	.023	.059	.054	.042	.036	.121
.144	.021	.013	.006	.010	.021	.066	.057	.035	.031	.144
.168	.009	-.001	-.011	-.010	-.010	.038	.031	.024	.021	.168
.217	.005	-.004	-.013	-.012	-.009	.043	.024	.015	.012	.217
.265	-.004	-.018	-.030	-.031	-.033	.014	.008	.002	-.001	.265
.361	-.011	-.024	-.037	-.040	-.050	-.020	-.013	-.014	-.015	.361
.409	-.007	-.021	-.033	-.034	-.060	-.038	-.025	-.025	-.025	.409
.457	-.014	-.028	-.042	-.044	-.061	-.049	-.021	-.021	-.022	.457
.502	-.014	-.027	-.040	-.042	-.067	-.067	-.033	-.031	-.028	.502
.578	-.010	-.023	-.036	-.036	-.066	-.074	-.038	-.038	-.033	.578
.626	-.010	-.024	-.037	-.039	-.068	-.075	-.050	-.045	-.040	.626
.674	.000	-.011	-.019	-.019	-.025	-.075	-.041	-.042	-.037	.674
.723	.006	-.007	-.014	-.014	.000	-.068	-.045	-.036	-.031	.723
.771	.017	.006	.000	.005	.017	-.075	-.052	-.042	-.038	.771
.795	.027	.017	.014	.020	.036	-.071	-.056	-.042	-.040	.795
.819	.037	.030	.027	.037	.056	-.054	-.056	-.039	-.037	.819
.843	.058	.054	.058	.071	.094	.053	-.031	-.038	-.036	.843
.853	.067	.065	.071	.083	.109	.106	-.023	-.032	-.032	.853
.863	.074	.073	.081	.097	.124	.142	-.015		-.028	.863

TABLE IV.- PRESSURE COEFFICIENTS FOR THE BODY WITH $A_{base}/A_{max} = 0.532$

(a) $l/d_{max} = 7$

x/l	C_p for M =												x/l
	0.60	0.80	0.90	0.95	1.00	1.03	1.20	1.61	2.01	2.50	2.96	3.95	
0.011	0.318	0.356	0.385	0.420	0.455	0.490	0.474	0.416	0.386	0.341	0.323	0.302	0.011
.017	.264	.296	.317	.347	.380	.417	.391	.341	.314	.270	.252	.236	.017
.024	.234	.262	.282	.313	.347	.383	.371	.291	.269	.229	.216	.198	.024
.038	.153	.170	.182	.208	.241	.281	.251	.226	.210	.184	.175	.159	.038
.056	.134	.151	.161	.185	.218	.259	.244	.201	.183	.154	.146	.128	.056
.084	.089	.098	.108	.129	.160	.200	.192	.159	.147	.122	.114	.098	.084
.111	.051	.052	.055	.071	.102	.142	.151	.129	.119	.098	.094	.082	.111
.139	.027	.025	.023	.038	.065	.103	.117	.103	.095	.078	.077	.068	.139
.167	.008	.005	-.001	.008	.034	.075	.082	.077	.073	.061	.060	.053	.167
.194	-.008	-.016	-.024	-.018	.003	.042	.052	.053	.054	.047	.046	.043	.194
.250	-.023	-.032	-.046	-.044	-.021	.018	.038	.038	.041	.029	.029	.028	.250
.306	-.037	-.046	-.063	-.065	-.048	-.014	.009	.020	.021	.013	.016	.019	.306
.361	-.049	-.064	-.083	-.093	-.084	-.054	-.022	-.004	.003	-.001	.003	.016	.361
.417	-.047	-.063	-.080	-.083	-.090	-.064	-.027	-.015	-.007	-.010	-.008	.001	.417
.472	-.059	-.075	-.098	-.107	-.112	-.089	-.050	-.027	-.018	-.019	-.017	-.006	.472
.528	-.063	-.081	-.106	-.133	-.142	-.119	-.070	-.041	-.031	-.030	-.020	-.008	.528
.584	-.057	-.071	-.093	-.106	-.140	-.121	-.075	-.053	-.039	-.037	-.034	-.017	.584
.667	-.048	-.060	-.080	-.093	-.153	-.139	-.088	-.066	-.053	-.043	-.039	-.022	.667
.722	-.049	-.060	-.080	-.091	-.172	-.157	-.112	-.079	-.061	-.054	-.046	-.029	.722
.778								-.069	-.057	-.055	-.048	-.029	.778
.833	-.005	-.009	-.019	-.016	-.123	-.122	-.087	-.067	-.057	-.055	-.049	-.031	.833
.889	.016	.013	.011	.020	.005	-.100	-.080	-.064	-.056	-.054	-.048	-.031	.889
.917	.031	.036	.035	.047	.078	-.065	-.064	-.052	-.047	-.051	-.045	-.031	.917
.944	.041	.046	.050	.063	.105	-.025	-.040	-.038	-.036				.944
.972	.047	.057	.064	.078	.121	.031	.013	-.016	-.023	-.031	-.031	-.018	.972
.983	.043	.052	.059	.073	.114	.039	.033	.009	-.003	-.018	-.022	-.017	.983
.994	.024	.031	.036	.050	.092	.029	.009	.010	.006	-.010	-.008	.005	.994

TABLE IV.- PRESSURE COEFFICIENTS FOR THE BODY WITH A_{base}/A_{max} = 0.532 - Continued

(b) l/d_{max} = 10

x/l	C_p for M =												x/l
	0.60	0.80	0.90	0.95	1.00	1.03	1.20	1.61	2.01	2.50	2.96	3.95	
0.009	0.201	0.220	0.239	0.259	0.298	0.307	0.274	0.255	0.222	0.200	0.183	0.174	0.009
.017	.158	.165	.175	.192	.229	.237	.208	.181	.169	.147	.134	.123	.017
.023	.149	.151	.164	.180	.218	.227	.211	.167	.149	.128	.117	.102	.023
.038	.123	.127	.131	.146	.182	.193	.194	.156	.125	.113	.102	.088	.038
.055	.089	.091	.091	.104	.137	.151	.140	.112	.103	.086	.082	.070	.055
.083	.057	.055	.055	.062	.094	.112	.111	.088	.081	.066	.063	.054	.083
.111	.038	.031	.026	.029	.057	.085	.077	.061	.056	.049	.045	.041	.111
.138	.032	.023	.019	.026	.053	.089	.076	.057	.048	.048	.042	.038	.138
.166	.014	.004	-.006	-.005	.016	.055	.053	.042	.036	.033	.032	.029	.166
.194	.010	-.004	-.012	-.013	.006	.050	.038	.032	.028	.026	.025	.023	.194
.222	.005	-.007	-.017	-.018	-.001	.045	.031	.026	.021	.022	.018	.018	.222
.249	-.004	-.014	-.026	-.027	-.003	.041	.023	.017	.014	.019	.015	.018	.249
.277	-.010	-.024	-.039	-.045	-.035	.009	.011	.007	.001	.009	.007	.014	.277
.305	-.010	-.023	-.038	-.042	-.035	.006	.003	.003	-.016	.004	.007	.007	.305
.416	-.022	-.041	-.057	-.067	-.069	-.043	-.026	-.019	-.020	-.011	-.014	-.004	.416
.472	-.022	-.041	-.057	-.065	-.077	-.060	-.037	-.025	-.022	-.013	-.017	-.008	.472
.528	-.021	-.040	-.056	-.065	-.079	-.071	-.032	-.025	-.026	-.020	-.022	-.011	.528
.583	-.015	-.031	-.047	-.052	-.078	-.079	-.037	-.031	-.035	-.025	-.027	-.011	.583
.666	-.020	-.036	-.051	-.059	-.086	-.089	-.053	-.042	-.039	-.025	-.027	-.016	.666
.722	-.014	-.031	-.046	-.051	-.087	-.097	-.065	-.047	-.035	-.033	-.032	-.018	.722
.778	.004	-.008	-.021	-.023	-.052	-.080	-.041	-.040	-.032	-.035	-.033	-.025	.778
.834	.014	.004	-.004	-.003	.035	-.072	-.047	-.036	-.028	-.034	-.033	-.025	.834
.889	.028	.020	.014	.018	.054	-.052	-.034	-.027	-.024	-.030	-.032	-.025	.889
.917	.036	.029	.023	.032	.064	-.040	-.031	-.022	-.018				.917
.945	.041	.037	.035	.044	.076	-.013	-.019	-.016	.002	-.021	-.024	-.016	.945
.972	.041	.040	.038	.049	.082	.026	.025	.009	.005	-.008	-.020	-.015	.972
.984	.028	.023	.021	.033	.064	.029	.019	.010	.003	-.001	-.011	.003	.984
.995	.004	-.002	.000	.010	.043	.035	-.031	-.001		-.002	-.013	-.009	.995

TABLE IV.- PRESSURE COEFFICIENTS FOR THE BODY WITH A_{base}/A_{max} = 0.532 - Concluded

(c) l/d_{max} = 13

x/l	C_p for M =												x/l
	0.60	0.80	0.90	0.95	1.00	1.03	1.20	1.61	2.01	2.50	2.96	3.95	
0.010	0.159	0.170	0.186	0.196	0.230	0.234	0.213	0.185	0.161	0.145	0.137	0.124	0.010
.016	.133	.133	.143	.150	.181	.185	.185	.160	.133	.118	.110	.095	.016
.023	.078	.073	.076	.077	.105	.108	.120	.112	.089	.077	.079	.068	.023
.038	.079	.076	.078	.077	.102	.114	.088	.070	.062	.054	.055	.045	.038
.055	.065	.062	.064	.062	.086	.105	.097	.081	.068	.053	.053	.043	.055
.083	.045	.039	.037	.033	.053	.078	.070	.060	.049	.038	.041	.034	.083
.111	.031	.024	.021	.014	.033	.056	.052	.042	.037	.028	.031	.029	.111
.139	.015	.003	-.004	-.013	-.002	.021	.034	.032	.026	.023	.024	.023	.139
.166	.012	.003	-.002	-.012	-.001	.008	.024	.020	.017	.020	.021	.016	.166
.194	.013	.004	-.001	-.010	.001	.010	.022	.018	.013	.013	.016	.013	.194
.221	.005	-.004	-.013	-.025	-.017	.000	.018	.014	.008	.011	.012	.009	.221
.250	.005	-.004	-.010	-.020	-.014	.013	.010	.010	.005	.008	.008	.005	.250
.278	.000	-.009	-.018	-.032	-.023	.017	.011	.004	.001	.003	.005	.004	.278
.305	-.005	-.017	-.028	-.040	-.037	.003	-.004	-.003	-.006	-.001	.002	.002	.305
.417	-.015	-.029	-.041	-.057	-.058	-.018	-.025	-.019	-.017	-.013	-.012	-.005	.417
.473	-.010	-.022	-.032	-.045	-.050	-.023	-.023	-.018	-.019	-.017	-.013	-.007	.473
.528	-.009	-.021	-.030	-.045	-.052	-.037	-.021	-.017	-.021	-.017	-.013	-.007	.528
.584	-.012	-.023	-.033	-.048	-.061	-.057	-.035	-.031	-.025	-.024	-.020	-.012	.584
.667	.000	-.009	-.018	-.030	-.040	-.064	-.025	-.024	-.026	-.023	-.020	-.014	.667
.723	.001	-.009	-.017	-.030	-.037	-.067	-.041	-.034	-.029	-.024	-.020	-.016	.723
.778	.014	.004	-.002	-.011	.009	-.046	-.020	-.026	-.023	-.028	-.023	-.016	.778
.833	.021	.013	.008	.000	.014	-.041	-.029	-.025	-.021	-.028	-.023	-.016	.833
.889	.030	.023	.020	.015	.031	-.033	-.025	-.021	-.020	-.025	-.023	-.016	.889
.917	.037	.031	.029	.026	.046	-.019	-.023	-.017	-.018				.917
.945	.040	.036	.037	.036	.057	-.002	-.015	-.009	-.010	-.016	-.016	-.014	.945
.972	.037	.033	.035	.036	.062	.024	.014	-.001	-.003	-.013	-.014	-.012	.972
.983	.034	.032	.032	.034	.060	.037	.023	.010	.005	-.005	-.008	.004	.983
.994	-.055	-.059	-.061	-.059	-.028	-.013	-.088	.048	.027	-.024	-.023	-.016	.994

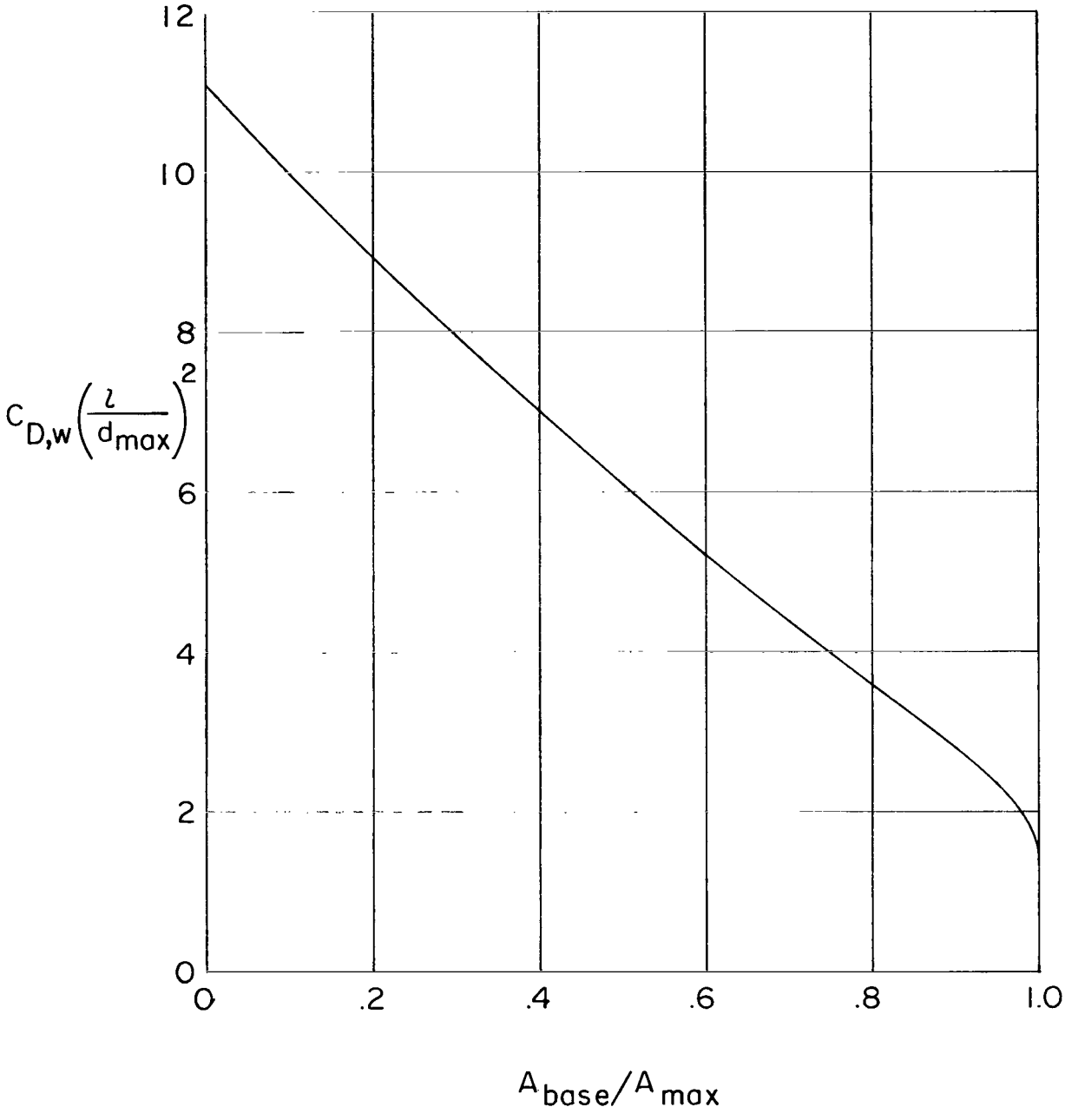

Figure 1.- Effects of afterbody closure and fineness ratio on wave drag of length-volume Haack-Adams bodies of revolution as predicted by slender-body theory.

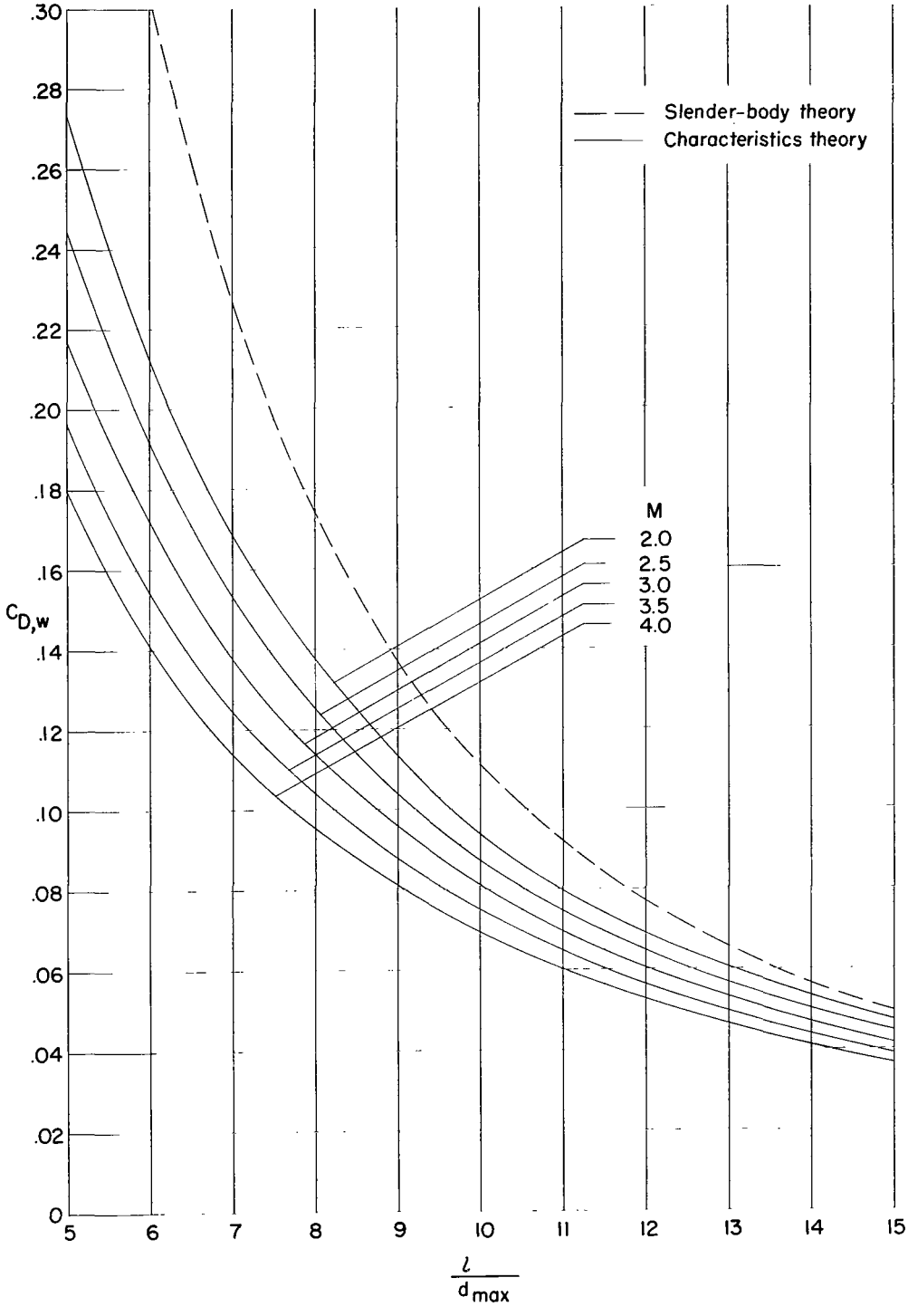

Figure 2.- Effects of Mach number on wave-drag variation with body fineness ratio. $A_{base}/A_{max} = 0$.

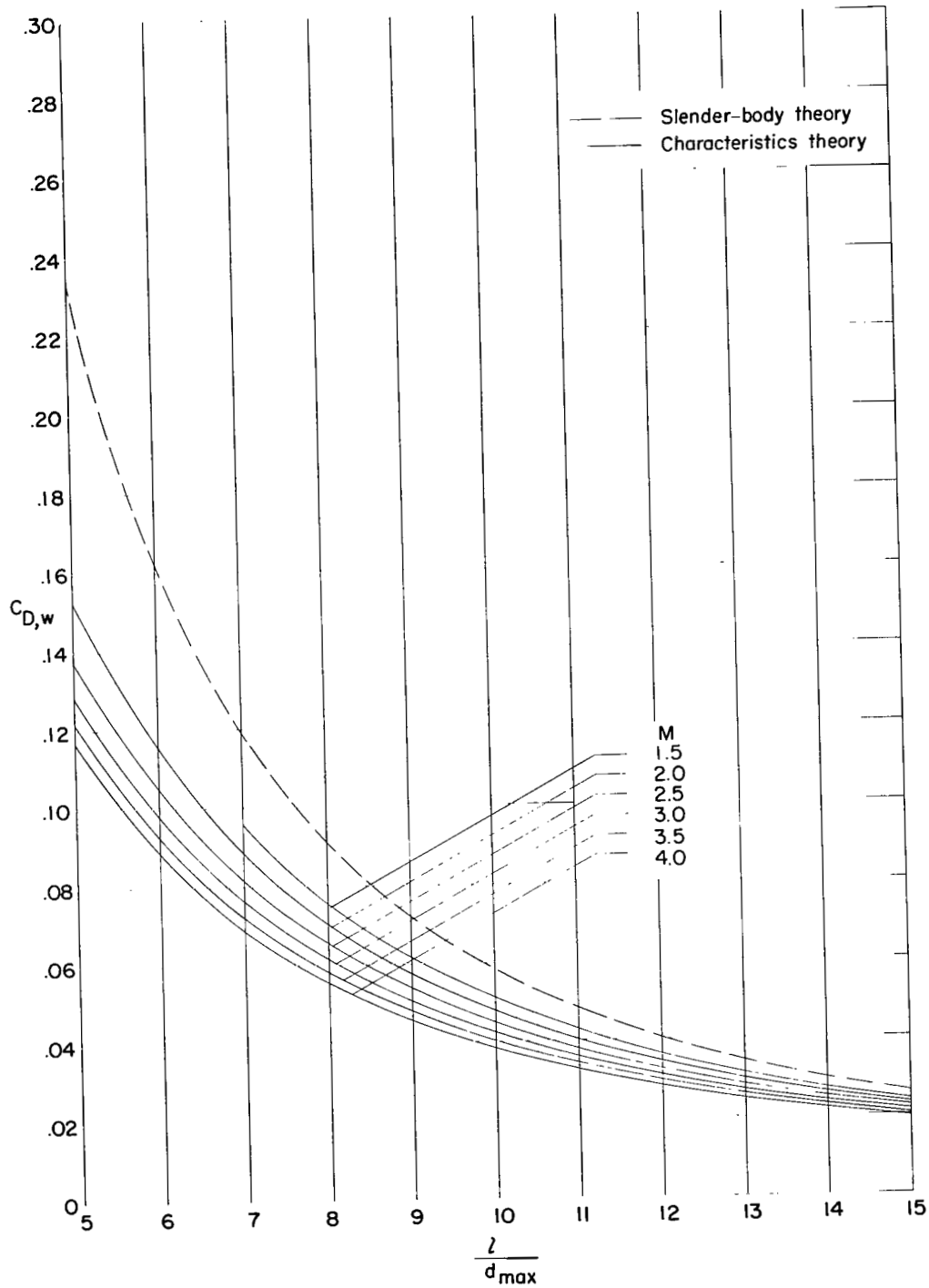

Figure 3.- Effects of Mach number on wave-drag variation with body fineness ratio. $A_{base}/A_{max} = 0.532$.

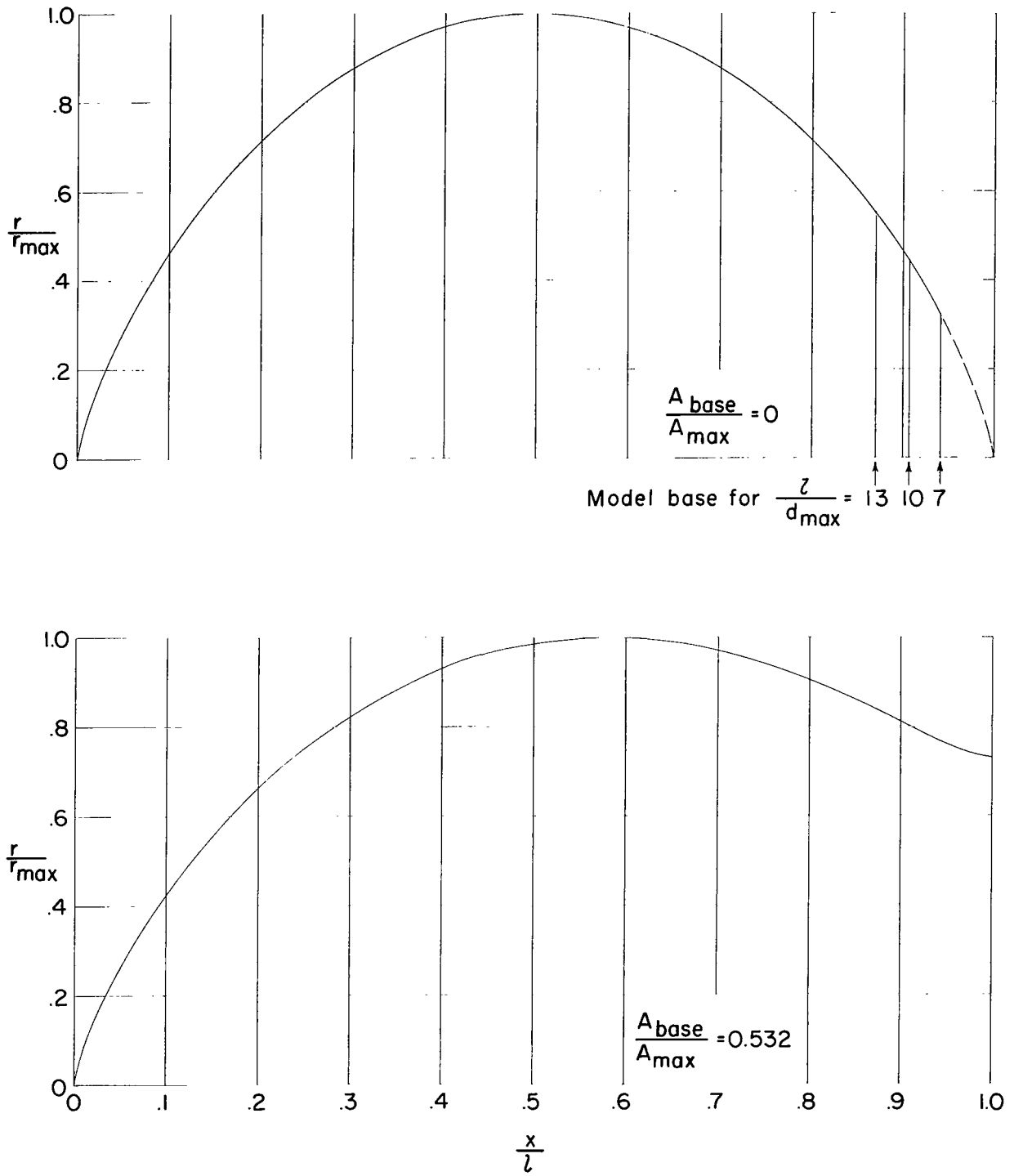

Figure 4.- Longitudinal distribution of body radii for the two series of length-volume Haack-Adams bodies of revolution.

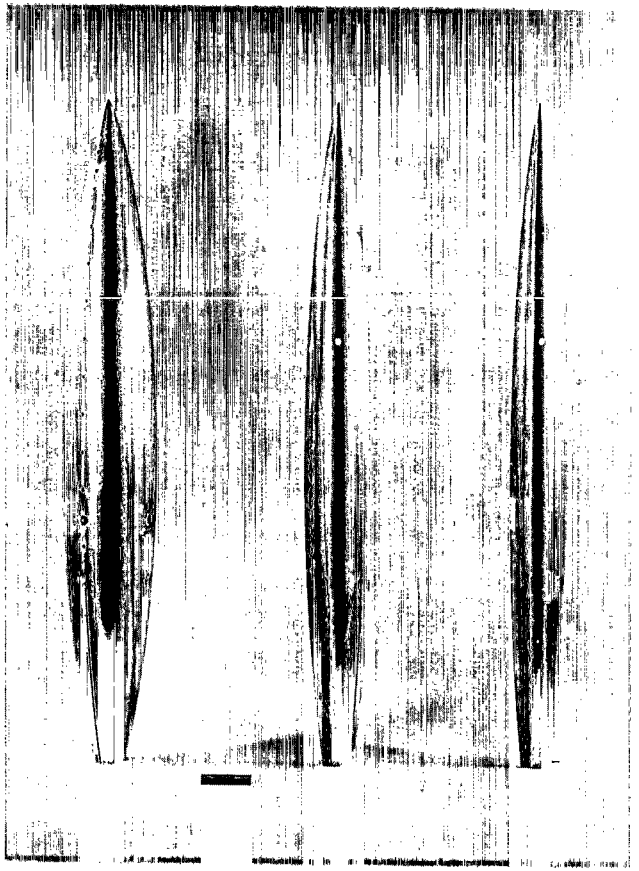

L-64-8462

(a) $A_{base}/A_{max} = 0.$

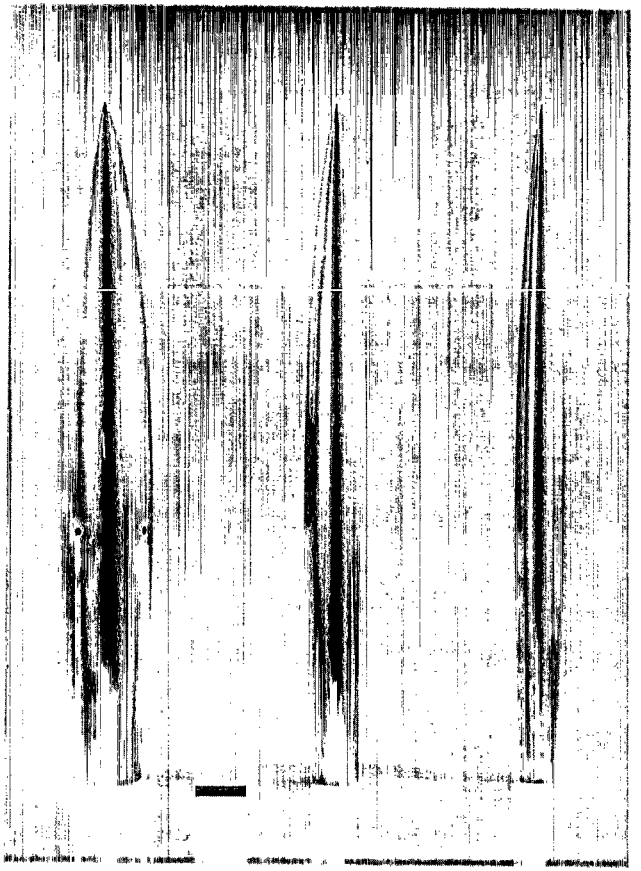

L-64-8461

(b) $A_{base}/A_{max} = 0.532.$

Figure 5.- Photographs of the models.

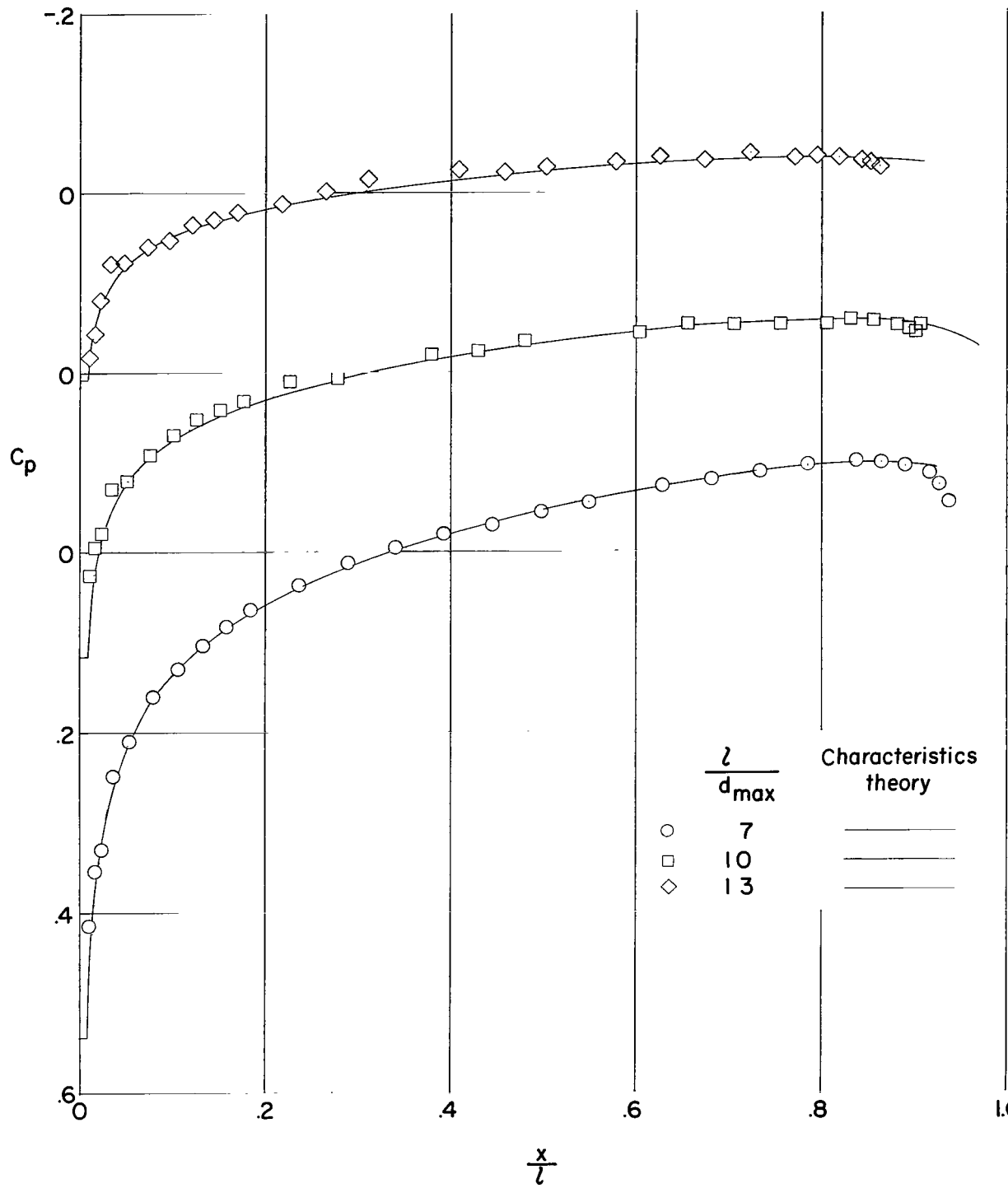

Figure 6.- Comparison of experimental pressure distributions with characteristics theory for the bodies with $A_{base}/A_{max} = 0$. M = 2.01.

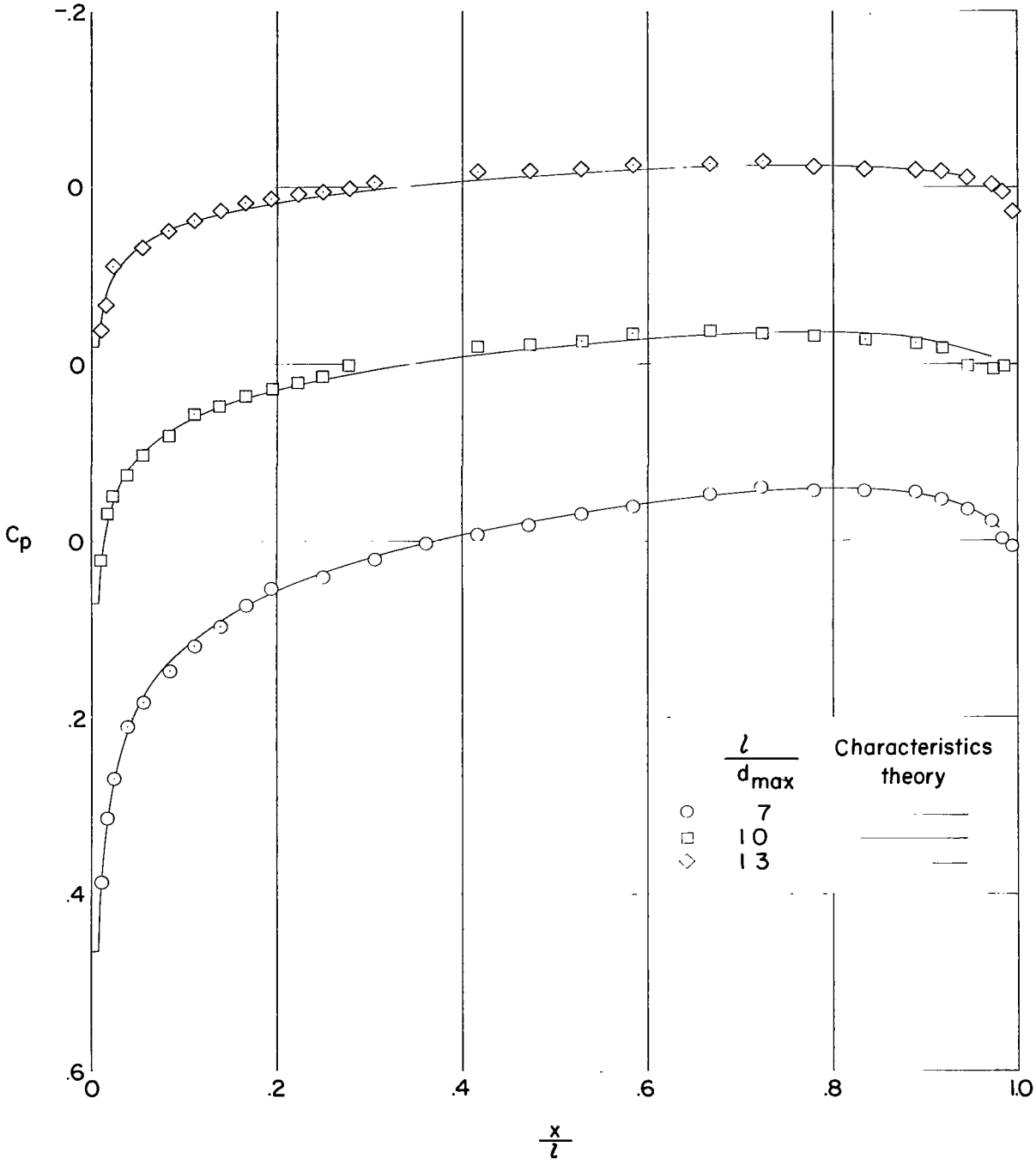

(a) M = 2.01.

Figure 7.- Comparison of experimental pressure distributions with characteristics theory for the bodies with $A_{base}/A_{max} = 0.532$.

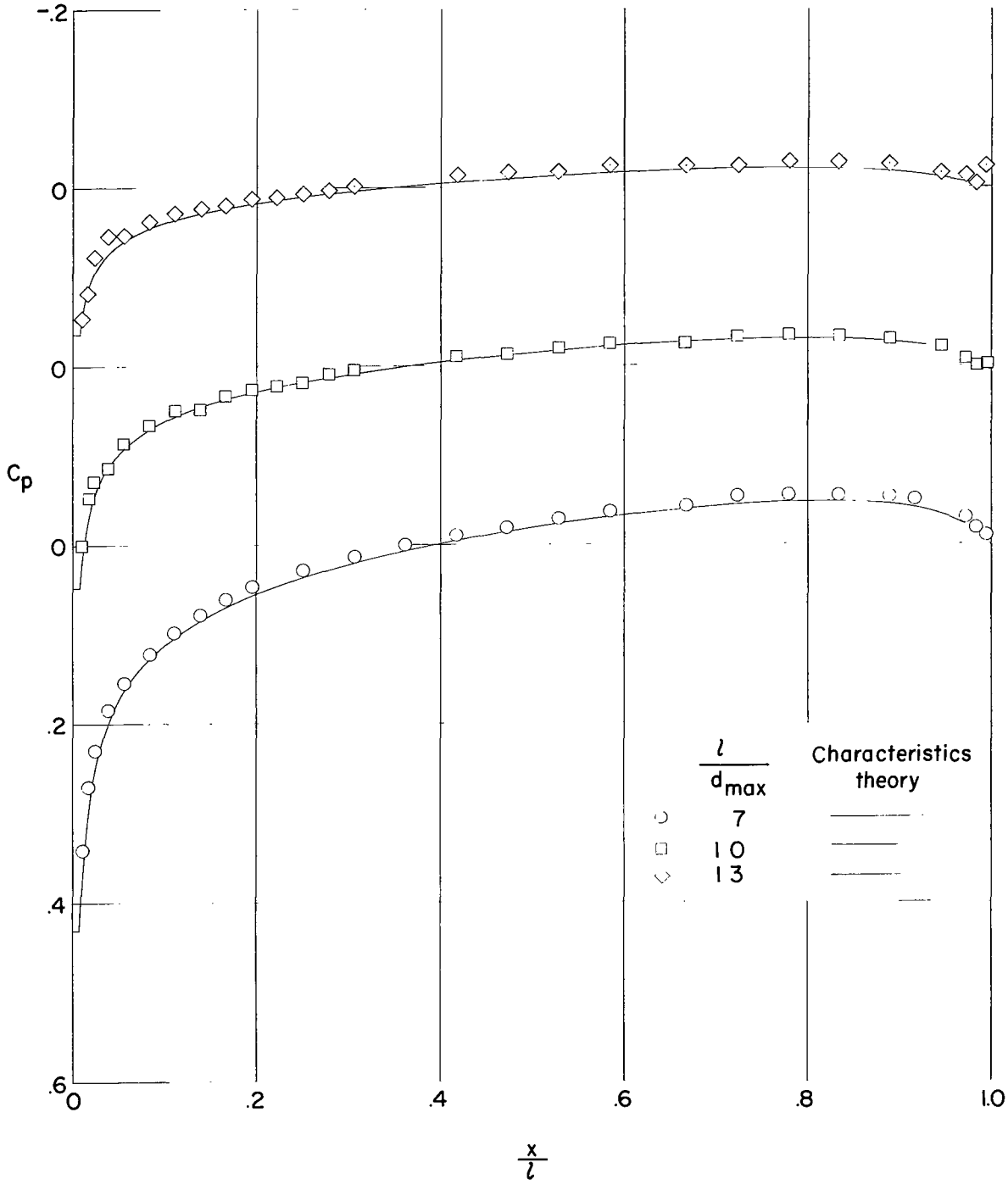

(b) M = 2.50.

Figure 7.- Continued.

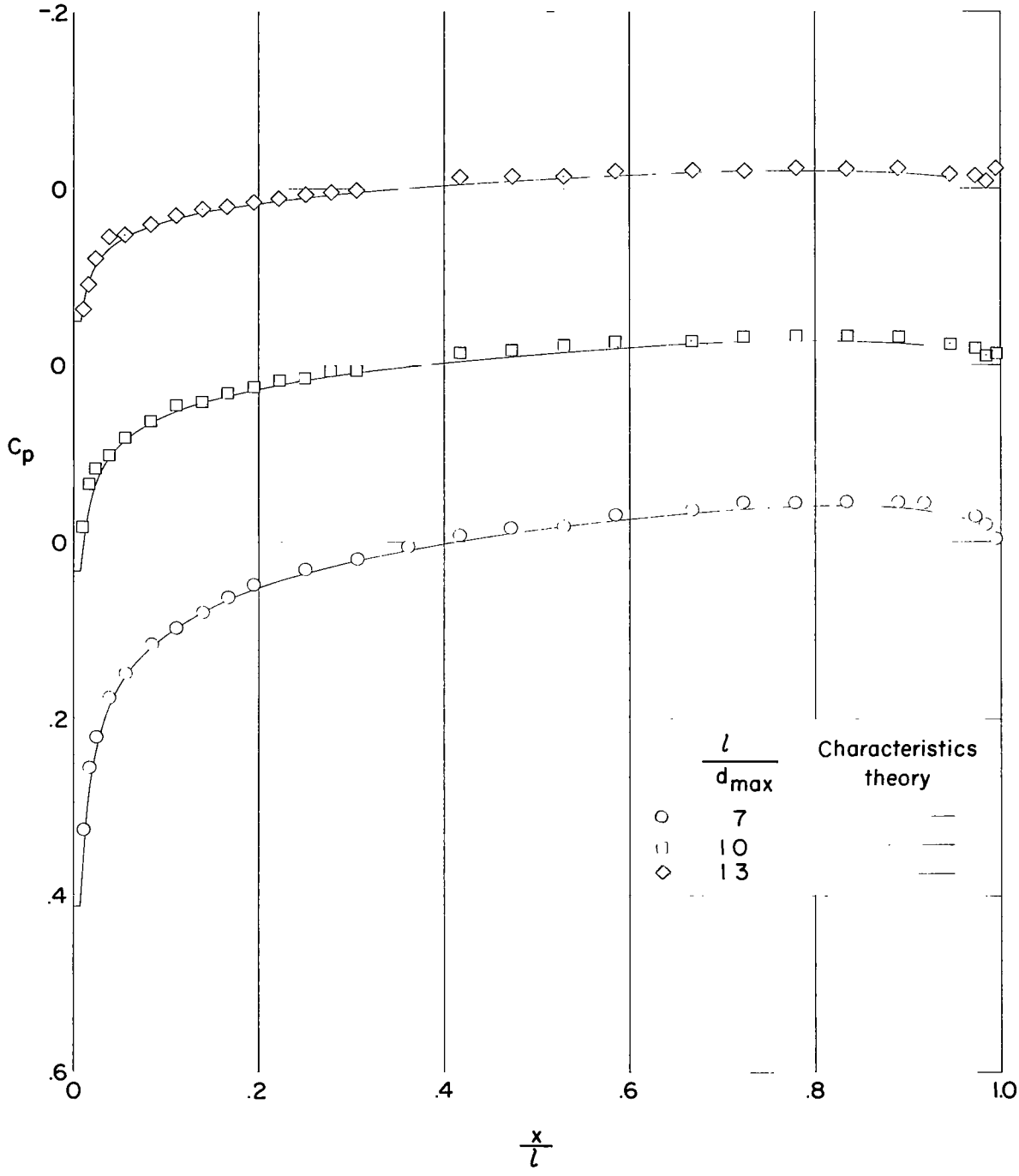

(c) M = 2.96.

Figure 7.- Continued.

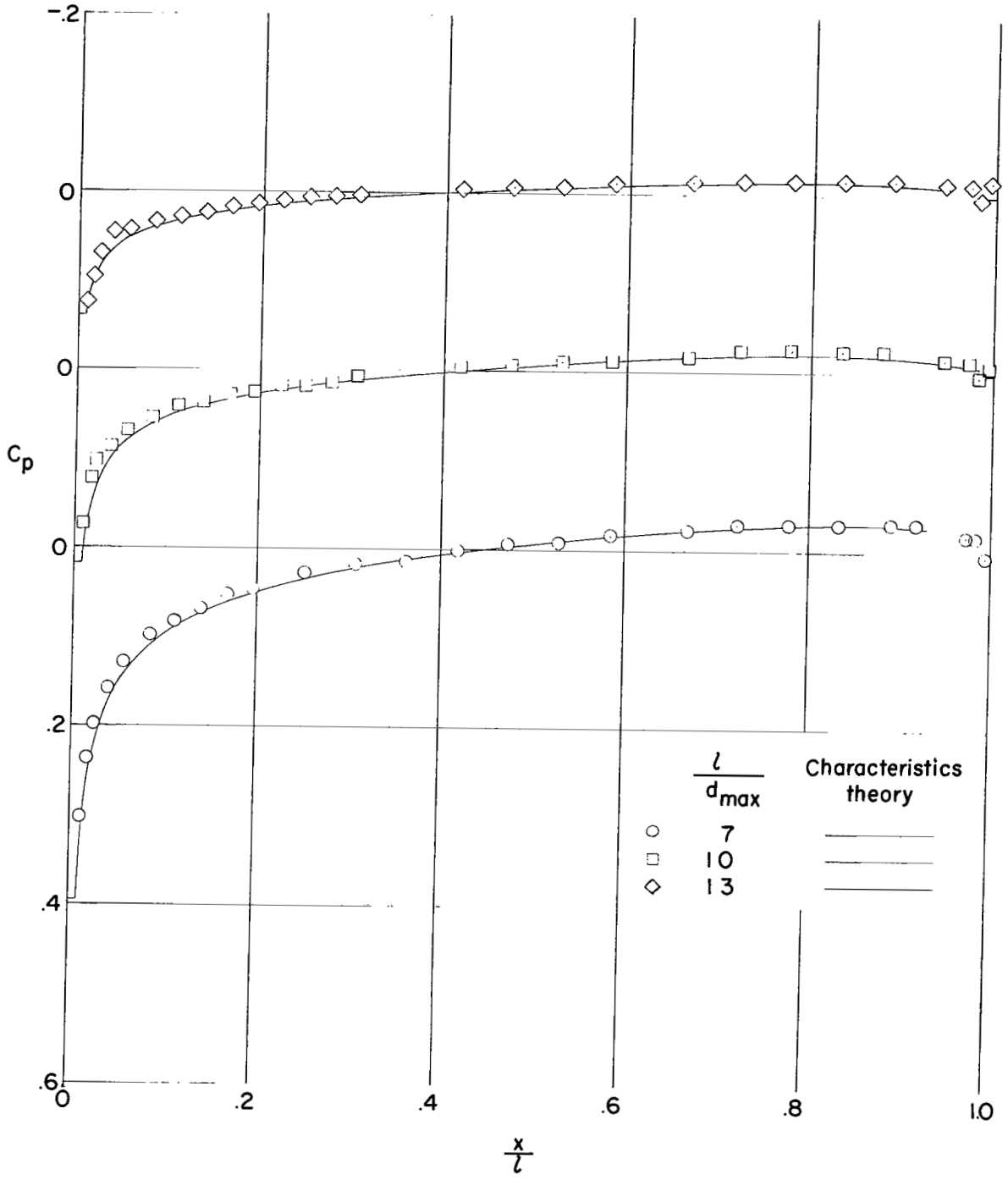

(d) M = 3.95.

Figure 7.- Concluded.

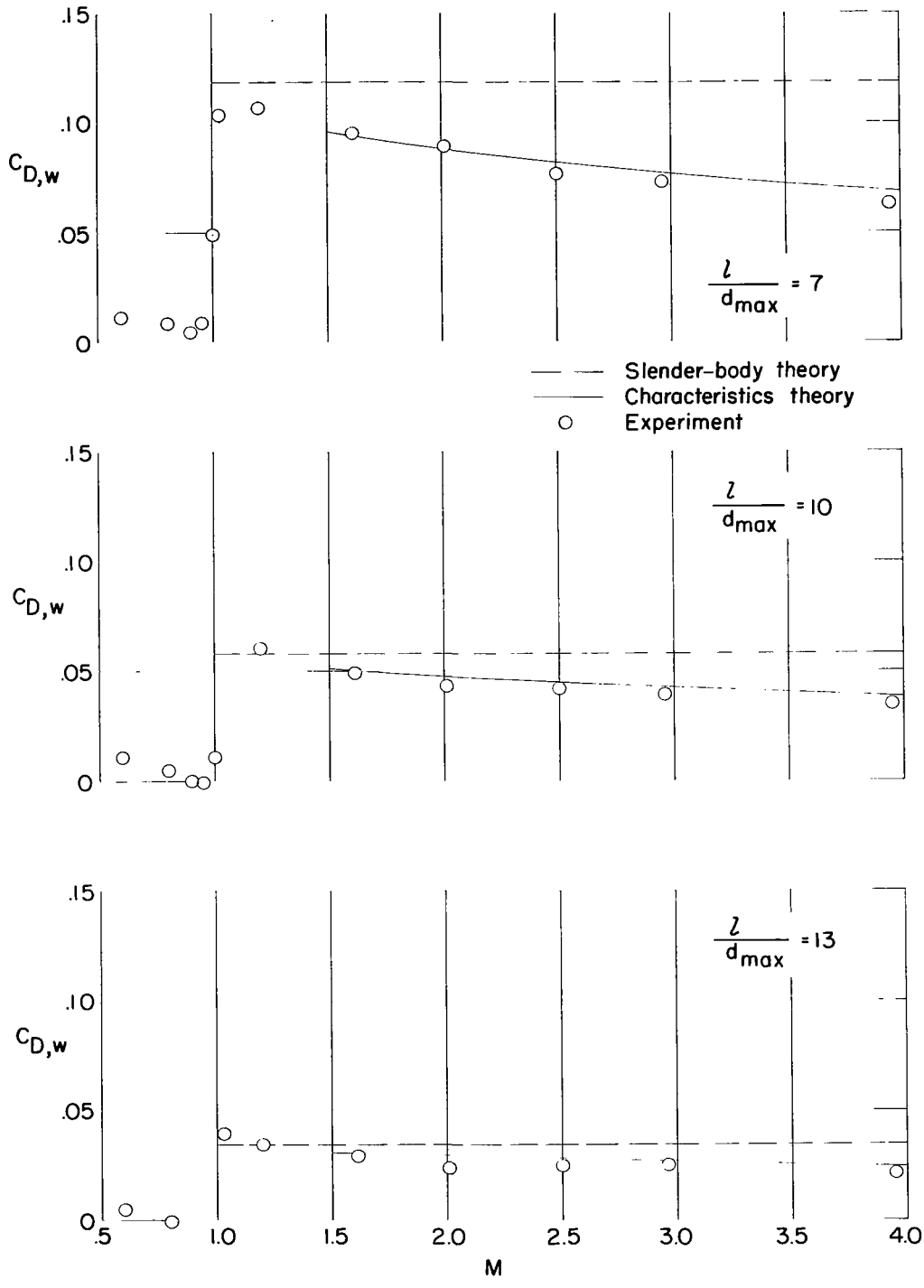

Figure 8.- Comparison of experimental wave-drag variations with slender-body theory and characteristics theory. $A_{base}/A_{max} = 0.532$.

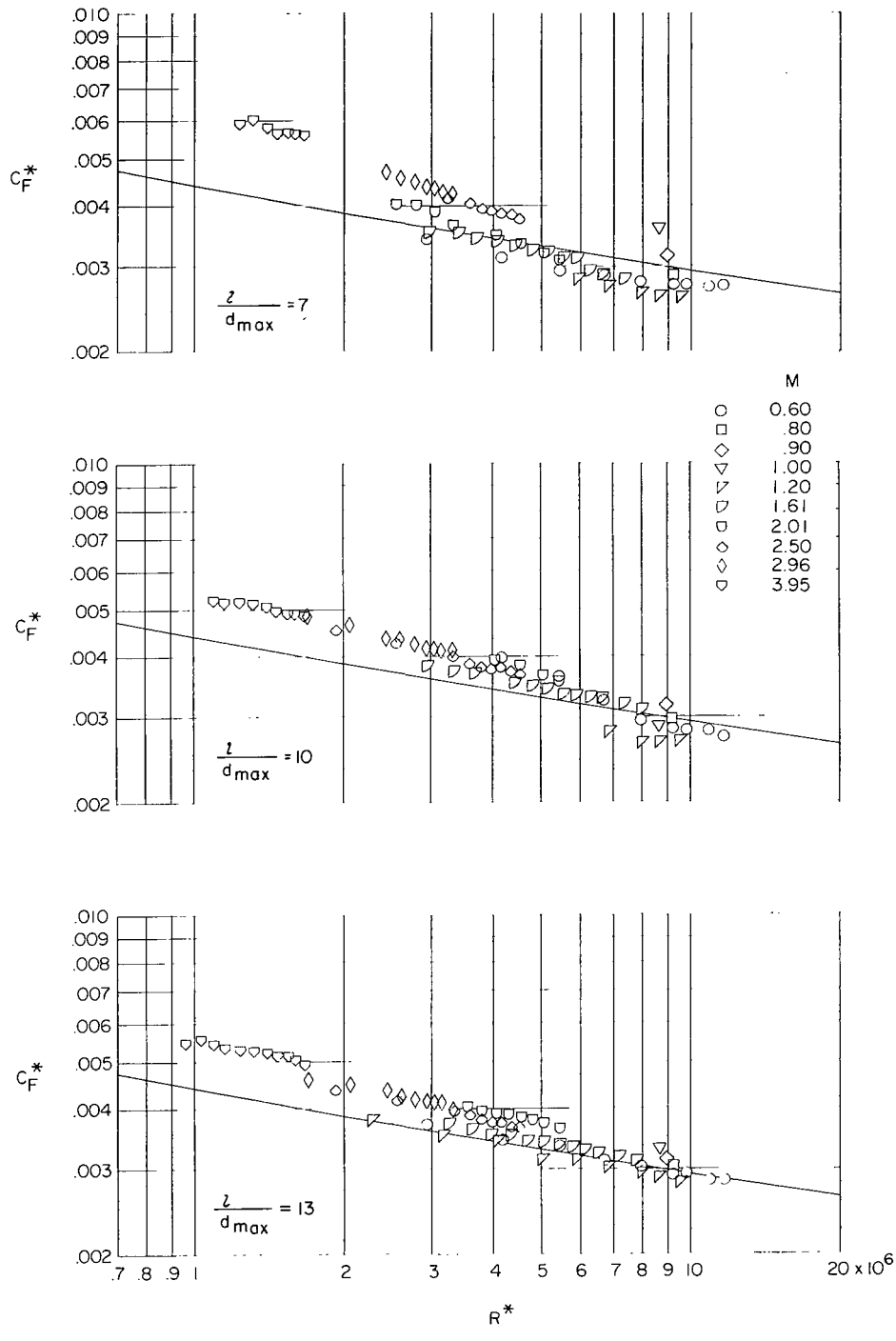

Figure 9.- Comparison of the transformed turbulent average skin-friction coefficients with the Kármán-Schoenherr incompressible curve for the bodies with $A_{base}/A_{max} = 0.532$.

"The aeronautical and space activities of the United States shall be conducted so as to contribute . . . to the expansion of human knowledge of phenomena in the atmosphere and space. The Administration shall provide for the widest practicable and appropriate dissemination of information concerning its activities and the results thereof."

—NATIONAL AERONAUTICS AND SPACE ACT OF 1958

NASA SCIENTIFIC AND TECHNICAL PUBLICATIONS

TECHNICAL REPORTS: Scientific and technical information considered important, complete, and a lasting contribution to existing knowledge.

TECHNICAL NOTES: Information less broad in scope but nevertheless of importance as a contribution to existing knowledge.

TECHNICAL MEMORANDUMS: Information receiving limited distribution because of preliminary data, security classification, or other reasons.

CONTRACTOR REPORTS: Technical information generated in connection with a NASA contract or grant and released under NASA auspices.

TECHNICAL TRANSLATIONS: Information published in a foreign language considered to merit NASA distribution in English.

TECHNICAL REPRINTS: Information derived from NASA activities and initially published in the form of journal articles.

SPECIAL PUBLICATIONS: Information derived from or of value to NASA activities but not necessarily reporting the results of individual NASA-programmed scientific efforts. Publications include conference proceedings, monographs, data compilations, handbooks, sourcebooks, and special bibliographies.

Details on the availability of these publications may be obtained from:

SCIENTIFIC AND TECHNICAL INFORMATION DIVISION

NATIONAL AERONAUTICS AND SPACE ADMINISTRATION

Washington, D.C. 20546